Supplementary information

A nickel(II)-based one-dimensional organic–inorganic halide perovskite ferroelectric with the highest Curie temperature

Hao-Fei Ni,‡[a] Lou-Kai Ye,‡[a] Peng-Cheng Zhuge,[a] Bo-Lan Hu,[a] Jia-Rui Lou,[a] Chang-Yuan Su,[b] Zhi-Xu Zhang,[b] Li-Yan Xie,*[a] Da-Wei Fu*[ab] and Yi Zhang*[ab]

[a]*Institute for Science and Applications of Molecular Ferroelectrics, Key Laboratory of the Ministry of Education for Advanced Catalysis Materials, Zhejiang Normal University, Jinhua, 321004, China. E-mail: liyanxie@zjnu.edu.cn, dawei@zjnu.edu.cn, yizhang1980@seu.edu*

[b]*Jiangsu Key Laboratory for Science and Applications of Molecular Ferroelectrics, Southeast University, Nanjing, 211189, China.*

‡ These authors have contributed equally to this work.

Experimental Measurement Methods

Single crystal X-ray crystallography

Variable-temperature X-ray single-crystal diffraction data of (3-pyrrolinium)$NiCl_3$ are collected using Mo Kα radiation (λ = 0.71073 Å) on a Rigaku Saturn 724 diffractometer at ω scan mode. Data processing, including empirical absorption correction, was performed by using the Crystal Clear software package. Crystal structures were resolved by direct method and continuous Fourier synthesis, and then refined by full-matrix least-squares methods based on F^2 with the SHELXLTL software package. All non-hydrogen atoms were refined anisotropically using all reflections with $I > 2\sigma(I)$, and the hydrogen atoms were generated geometrically at appropriate position. Moreover, calculations involving the angles and distances between some atoms were measured by DIAMOND and SHELXLTL. Crystallographic data and structure refinement of (3-pyrrolinium)$NiCl_3$ at 293 and 453 K are listed in Table S1. CCDC 2214383-2214384 for the compounds contains the supplementary crystallographic data for this article. These data can be obtained free of charge from The Cambridge Crystallographic Data Centre via www.ccdc.cam.ac.uk/ data_request/cif.

Differential scanning calorimetry and dielectric measurements

Differential scanning calorimetry (DSC) measurements were performed on a NETZSCH DSC 214 instrument. The crystalline samples of the two compounds were measured with a rate of 10 K min^{-1} under a nitrogen atmosphere. The complex dielectric permittivity curves were measured on an automatic impedance Tonghui 2828 analyzer in the frequency range from 500 Hz to 1 MHz with an applied voltage of 1.0 V. Dielectric studies were performed on pressed-powder pellets and single crystal samples, and conductive carbon/silver glue was deposited on the surface of electrode to simulate parallel plate capacitors.

SHG measurements. An unexpanded laser beam with low divergence (pulsed Nd:YAG at a wavelength of 1064 nm, 5 ns pulse duration, 1.6 MW peak power, 10 Hz repetition rate) was used to perform the second harmonic generation (SHG) experiments. The instrument model is Ins 1210058, INSTEC Instruments, while the laser is Vibrant 355 II, OPOTEK.

Hirshfeld surfaces analysis. Hirshfeld surfaces were calculated by using the CrystalExplorer program with inputting structure file in CIF format. In this work, all the Hirshfeld surfaces were generated using a standard (high) surface resolution. The intensity of molecular interaction is mapped onto the Hirshfeld surface by using the respective red-blue-white scheme: where the white or green regions exactly correspond to the distance of Van der Waals contact, the blue regions correspond to longer contacts, and the red regions represent closer contacts. The normalized contact distance d_{norm} is based on d_e, d_i and the van der Waals (vdW) radii of the two atoms external (r_e^{vdW}) and internal (r_i^{vdW}) to the surface:

$$d_{norm} = \frac{d_i - r^{vdW}}{r_i^{vdW}} + \frac{d_e - r}{r_e^{vdW}}$$

d_{norm} surface is used for the identification of close intermolecular interaction.

Density Functional Theory Calculations. The Density functional theory were carried out with the Vienna Ab Initio Simulation Package (VASP)[1]. The projector-augmented wave method (PAW)[2] and Perdew-Burke-Ernzerhof (PBE)[3] functional were used to describe the electron-ion and the exchange-correlation interactions respectively. The energy barrier for the rotation of 3-pyrrolinimu cations were calculated based on crystal structures of the (3-pyrrolinium)$CdCl_3$, (3-pyrrolinium)$MnCl_3$ and (3-

pyrrolinium)$NiCl_3$ and therefore no optimization by structural relaxation is required. A cutoff energy of 500 eV was adopted for all simulations and the energy convergence criteria was set to 10^{-5} eV. The Brillouin zone was sampled using a Monkhorst-Pack mesh of 1*1*1 k-point grids for energy calculations.

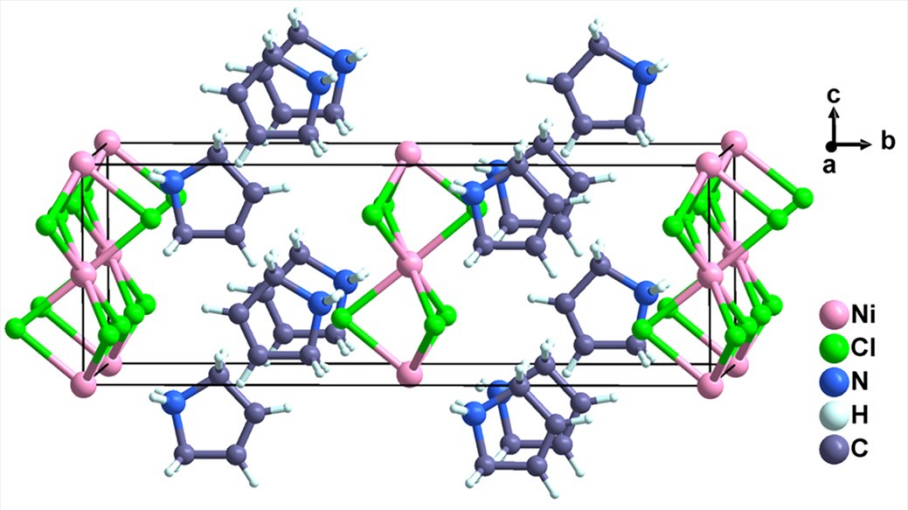

Fig. S1 The point charge model for (3-pyrrolinium)$NiCl_3$ at 293 K in LTP.

According to the crystal structure data collected at 293 K, we select a unit cell and assume that the centers of the positive charges of the 3-pyrrolinium cations and the negative charges of the $(NiCl_3)^-$ chains are located on the N atoms and Ni atoms, respectively.

Atoms	Coordinate of charge center
Ni	(0.5, 0.5, 0.3854)
N	(0.5, 0.5, 0.5059)

$$P_s = \lim \frac{1}{V} \sum q_i r_i$$

$= (q_{Ni}r_{Ni} + q_N r_N) / V$
$= [(-e \times 0.3854) + (e \times 0.5059] \times 4 \times c / V$
$= [0.1205 \times 4 \times 1.6 \times 10^{-19} \times 6.177 \times 10^{-10}\ \text{C m}] / (783.0 \times 10^{-30}\ \text{m}^3)$
$= 6.08 \times 10^{-2}\ \text{C m}^{-2}$
$|P_s| = 6.08 \times 10^{-2}\ \text{C m}^{-2} = 6.08\ \mu\text{C cm}^{-2}$

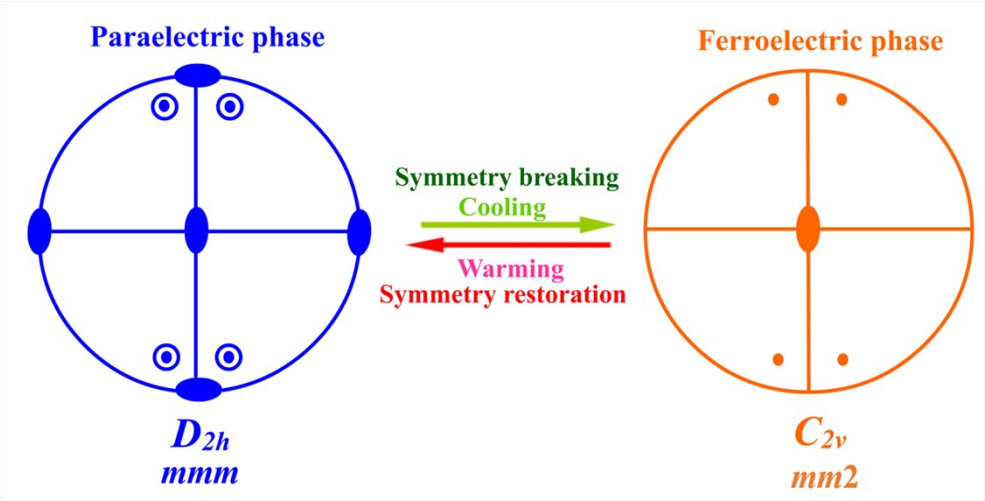

Fig. S2 Equatorial plane projection of point group of D_{2h} in the paraelectric phase and C_{2v} in in the ferroelectric phase.

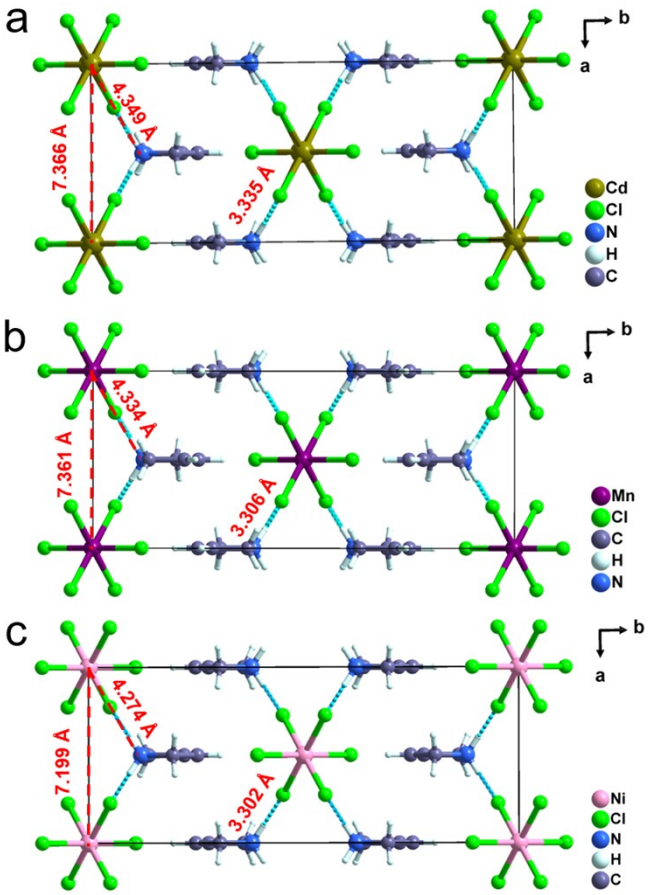

Fig. S3 Structural packing diagrams of (a) (3-pyrrolinium)$CdCl_3$, (b) (3-pyrrolinium)$MnCl_3$ and (c) (3-pyrrolinium)$NiCl_3$ in their respective ferroelectric phase. The sky blue dotted lines represent N−H···Cl hydrogen bonding.

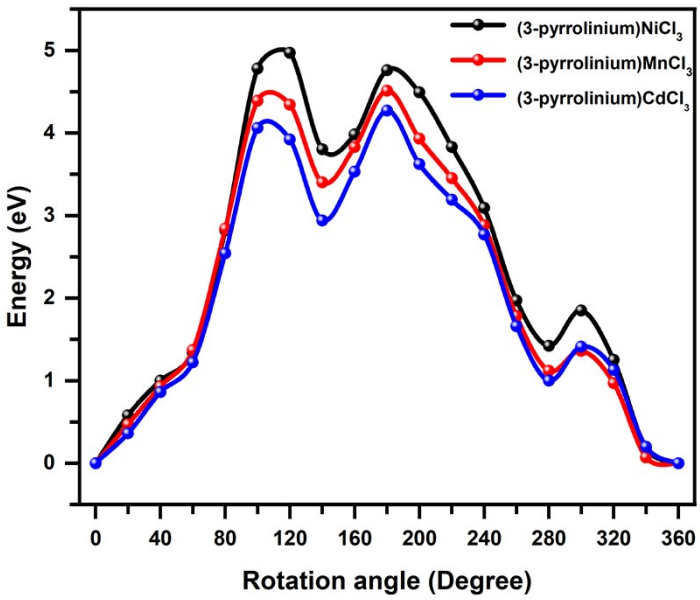

Fig. S4 The Energy barrier for the rotation of 3-pyrrolinium cations in (3-pyrrolinium)MCl3(M=Ni, Cd, Mn).

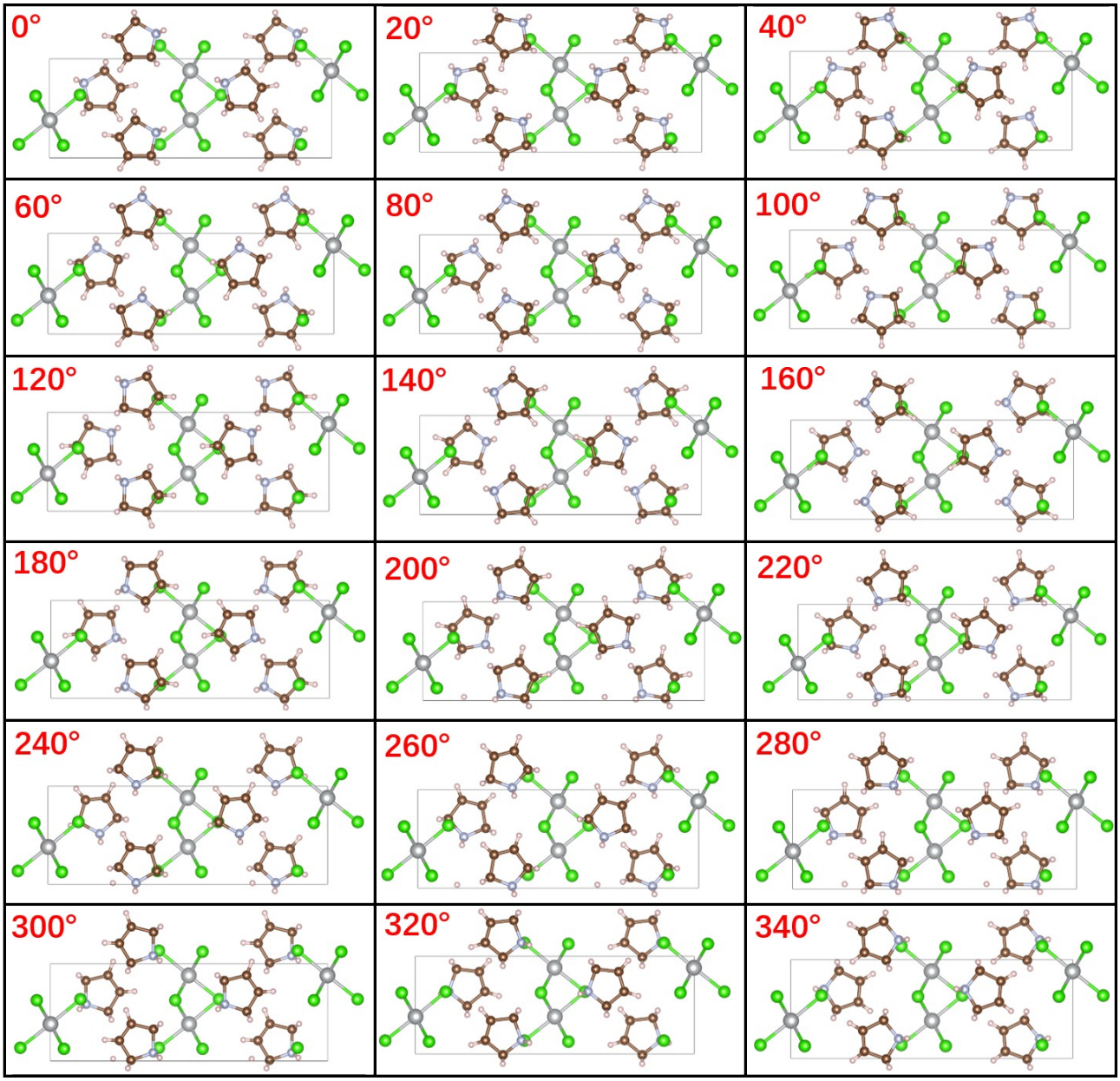

Fig. S5 The Computational models of the energy barrier for the rotation of (3-pyrrolinium)$NiCl_3$.

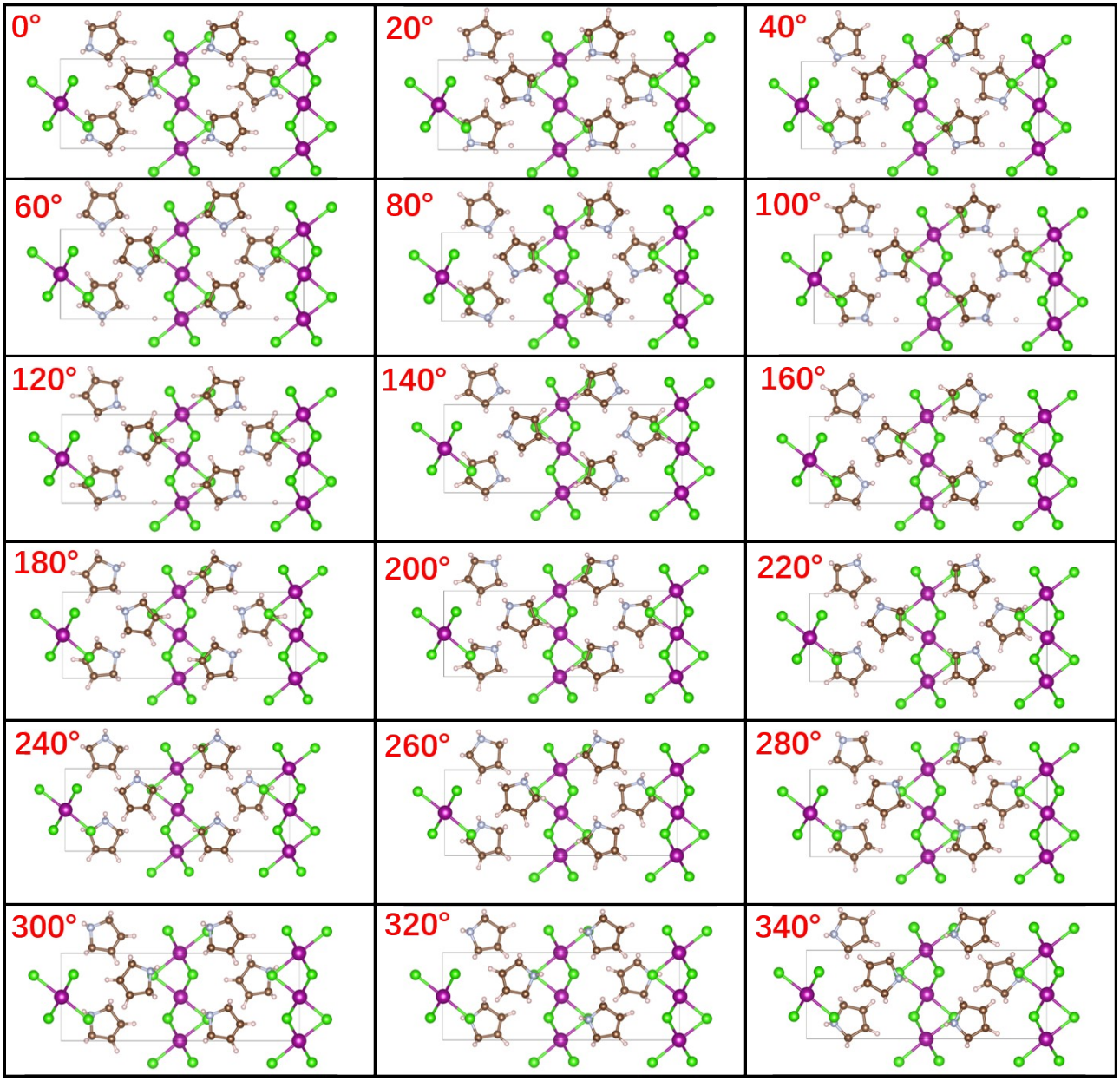

Fig. S6 The Computational models of the energy barrier for the rotation of (3-pyrrolinium)$MnCl_3$.

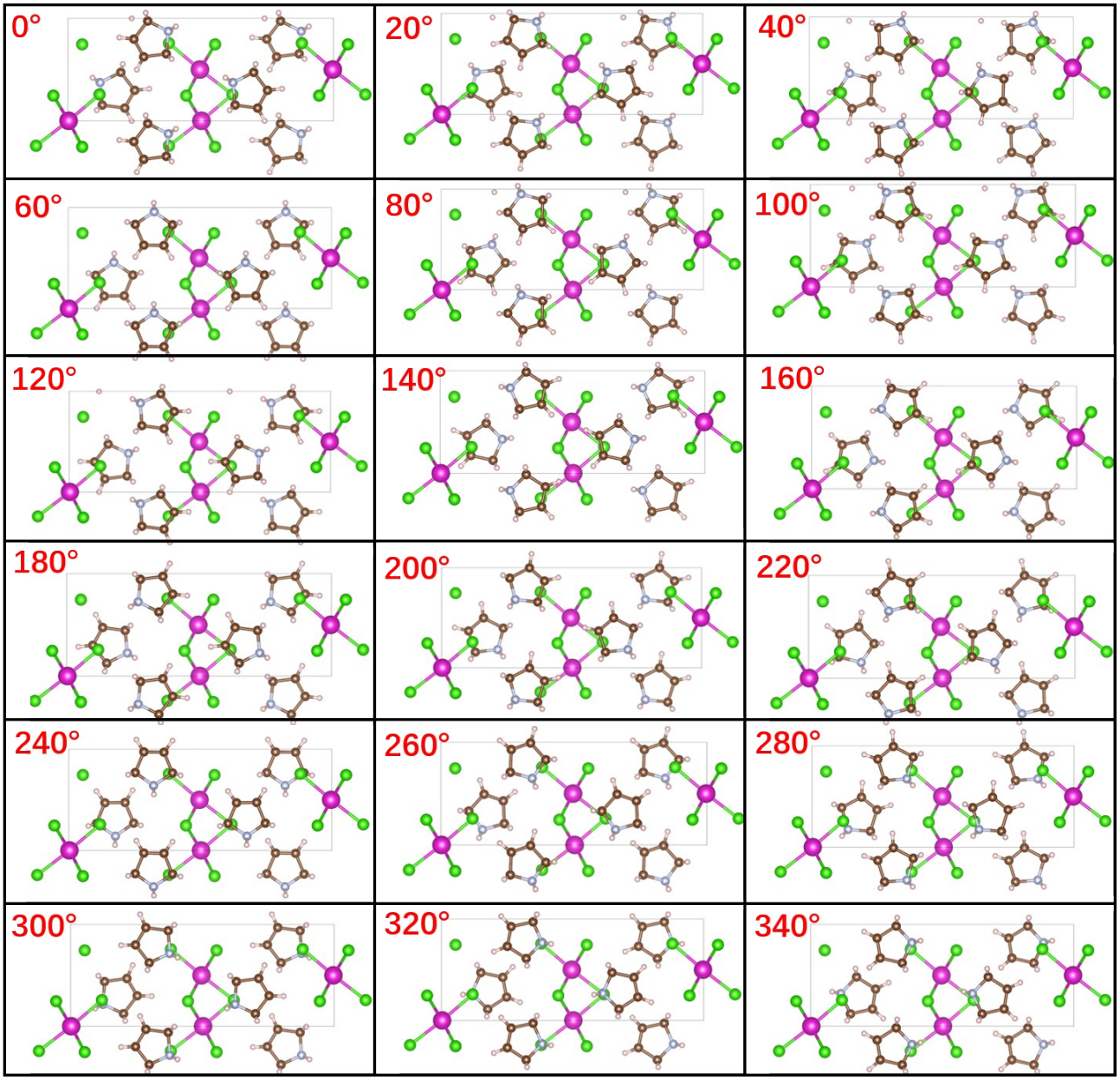

Fig. S7 The Computational models of the energy barrier for the rotation of (3-pyrrolinium)$CdCl_3$.

Table S1. Crystal data and structure refinement for (3-pyrrolinium)$NiCl_3$ at 293 K and 453 K.

Compound	(3-pyrrolinium)$NiCl_3$	
Temperature	293 K	453 K
Formula	$(C_4H_8N)NiCl_3$	$(C_4H_8N)NiCl_3$
Weight	235.17	235.17
System	orthorhombic	orthorhombic
Space group	$Cmc2_1$	*Cmcm*
a (Å)	7.1992(17)	7.35(3)
b (Å)	17.607(5)	17.78(7)
c (Å)	6.1770(14)	6.23(2)
α (°)	90	90
β (°)	90	90
γ (°)	90	90
V (Å^3)	783.0(3)	814(6)
Z	4	4
R_{int}	0.0440	0.0689
R_1	0.0337	0.0612
wR_2	0.0607	0.1863
GOF	1.081	1.006

Table S2. The void volume of (3-pyrrolinium)$CdBr_3$, (3-pyrrolinium)$CdCl_3$, (3-pyrrolinium)$MnCl_3$ and (3-pyrrolinium)$NiCl_3$. ($V_{void} = V_{cell} - 4V_{octahedron}$). There are four completed octahedrons in a unit cell and the octahedron volume was calculated by DIAMOND software.

	(3-pyrrolinium)$CdBr_3$ (T_c = 237.9 K)	(3-pyrrolinium)$CdCl_3$ (T_c = 316 K)	(3-pyrrolinium)$MnCl_3$ (T_c = 376 K)	(3-pyrrolinium)$NiCl_3$ (T_c = 428 K)
Cell volume (Å^3)	942.1	851.7	832.4	783.0
Octahedron volume (Å^3)	28.2	23.9	21.8	18.6
void volume (Å^3)	829.3	756.1	745.2	708.6

Table S3. The energy barrier for the different rotation angles of (3-pyrrolinium)MCl_3 (M=Ni, Cd, Mn). (Maximum values are marked in red)

Rotation angle (Degree)	Energy for Ni (eV)	Energy for Mn (eV)	Energy for Cd (eV)
0	0	0	0
20	0.58	0.47	0.36
40	1	0.93	0.86
60	1.34	1.37	1.22
80	2.82	2.84	2.54
100	4.78	4.39	4.06
120	4.97	4.34	3.92
140	3.8	3.4	2.94
160	3.98	3.83	3.53
180	4.76	4.51	4.27
200	4.49	3.93	3.62
220	3.83	3.45	3.19
240	3.09	2.88	2.77
260	1.97	1.78	1.66
280	1.42	1.12	1
300	1.85	1.36	1.41
320	1.25	0.97	1.13
340	0.18	0.07	0.2
360	0	0	0

Table S4. The comparison of saturated polarization (P_s) and Curie temperature (T_c) in reported ABX_3-type one-dimensional organic–inorganic halide perovskite ferroelectrics.

Compound	P_s (μC cm^{-2})	T_c (K)	Ref
$N(CH_3)_4CdBr_3$	0.12	156	4
(1-azabicyclo[2.2.1]heptane)$CdCl_3$	-	190	5
(pyrrolidinium)$MnBr_3$	6.0	219	6
(3-pyrrolinium)$CdBr_3$	5.65	237.9	7
(pyrrolidinium)$CdCl_3$	3.6	218-240	8
(*R*)-3-(fluoropyrrolidinium)$MnBr_3$	4.8	273	9
(*S*)-3-(fluoropyrrolidinium)$MnBr_3$	4.5	273	9
$(C_5H_9NH_3)CdCl_3$	1.7	285	10
(pyrrolidinium)$MnCl_3$	5.5	295	11
(*R*)-3-(fluoropyrrolidinium)$CdCl_3$	5.63	303	12
(*S*)-3-(fluoropyrrolidinium)$CdCl_3$	5.79	303	12
$[(CH_3)_3NCH_2I]PbI_3$	-	312	13
(3-pyrrolinium)$CdCl_3$	5.1	316	14
(*R*)-3-(fluoropyrrolidinium)$MnCl_3$	5.0	333	15
(*S*)-3-(fluoropyrrolidinium)$MnCl_3$	5.4	333	15
$[(CH_3)_3NCH_2Cl)]CdBr_3$	3.5	346	16
$[(CH_3)_4P]CdCl_3$	0.43	348	17
(*R*)-3-OH-$(C_4H_9N)[CdCl_3]$	2.1	350	18
(*S*)-3-OH-$(C_4H_9N)[CdCl_3]$	-	350	18
(3-pyrrolinium)$MnCl_3$	6.2	376	19
$[(CH_3)_3NCH_2Cl)]CrCl_3$	3.6	397	20
$[(CH_3)_3NCH_2Cl)]MnCl_3$	4.0	406	21
(4-fluoro-1-azabicyclo[2.2.1]heptane)$CdCl_3$	11.2	419	5
(3-pyrrolinium)$NiCl_3$	5.8	428	This work

Reference

1. G. Kresse and J. Furthmüller, *Comput. Mater. Sci.*, 1996, **6**, 15-50.
2. P. E. Blochl, *Phys. Rev. B*, 1994, **50**, 17953-17979.
3. J. P. Perdew, M. Ernzerhof and K. Burke, *J. Chem. Phys.*, 1996, **105**, 9982-9985.
4. K. Gesi, *J. Phys. Soc. Jpn.*, 1990, **59**, 432-434.
5. Y.-Y. Tang, Y. Xie, Y.-L. Zeng, J.-C. Liu, W.-H. He, X.-Q. Huang and R.-G. Xiong, *Adv. Mater.*, 2020, **32**, 2003530.
6. Y. Zhang, W. Q. Liao, D. W. Fu, H. Y. Ye, C. M. Liu, Z. N. Chen and R. G. Xiong, *Adv. Mater.*, 2015, **27**, 3942-3946.
7. P. F. Li, W. Q. Liao, Y. Y. Tang, H. Y. Ye, Y. Zhang and R. G. Xiong, *J. Am. Chem. Soc.*, 2017, **139**, 8752-8757.
8. W.-J. Xu, C.-T. He, C.-M. Ji, S.-L. Chen, R.-K. Huang, R.-B. Lin, W. Xue, J.-H. Luo, W.-X. Zhang and X.-M. Chen, *Adv. Mater.*, 2016, **28**, 5886-5890.
9. J.-X. Gao, W.-Y. Zhang, Z.-G. Wu, Y.-X. Zheng and D.-W. Fu, *J. Am. Chem. Soc.*, 2020, **142**, 4756-4761.

10. Y. Zhang, H.-Y. Ye, W. Zhang and R.-G. Xiong, *Inorg. Chem.Front.*, 2014, **1**, 118-123.
11. Y. Zhang, W. Q. Liao, D. W. Fu, H. Y. Ye, Z. N. Chen and R. G. Xiong, *J. Am. Chem. Soc.*, 2015, **137**, 4928-4931.
12. Y.-Y. Tang, Y. Ai, W.-Q. Liao, P.-F. Li, Z.-X. Wang and R.-G. Xiong, *Adv. Mater.*, 2019, **31**, 1902163.
13. X.-N. Hua, W.-Q. Liao, Y.-Y. Tang, P.-F. Li, P.-P. Shi, D. Zhao and R.-G. Xiong, *J. Am. Chem. Soc.*, 2018, **140**, 12296-12302.
14. H. Y. Ye, Y. Zhang, D. W. Fu and R. G. Xiong, *Angew. Chem., Int. Ed.*, 2014, **53**, 11242-11247.
15. Y. Ai, X.-G. Chen, P.-P. Shi, Y.-Y. Tang, P.-F. Li, W.-Q. Liao and R.-G. Xiong, *J. Am. Chem. Soc.*, 2019, **141**, 4474-4479.
16. W. Q. Liao, Y. Y. Tang, P. F. Li, Y. M. You and R. G. Xiong, *J. Am. Chem. Soc.*, 2018, **140**, 3975-3980.
17. L. Zhou, P.-P. Shi, X.-M. Liu, J.-C. Feng, Q. Ye, Y.-F. Yao, D.-W. Fu, P.-F. Li, Y.-M. You, Y. Zhang and R.-G. Xiong, *NPG Asia Mater.*, 2019, **11**, 15.
18. H. Ye, W.-H. Hu, W.-J. Xu, Y. Zeng, X.-X. Chen, R.-K. Huang, W.-X. Zhang and X.-M. Chen, *APL Mater.*, 2021, **9**, 031102.
19. H. Y. Ye, Q. Zhou, X. Niu, W. Q. Liao, D. W. Fu, Y. Zhang, Y. M. You, J. Wang, Z. N. Chen and R. G. Xiong, *J. Am. Chem. Soc.*, 2015, **137**, 13148-13154.
20. Y. Ai, R. Sun, Y.-L. Zeng, J.-C. Liu, Y.-Y. Tang, B.-W. Wang, Z.-M. Wang, S. Gao and R.-G. Xiong, *Chem. Sci.*, 2021, **12**, 9742-9747.
21. Y.-M. You, W.-Q. Liao, D. Zhao, H.-Y. Ye, Y. Zhang, Q. Zhou, X. Niu, J. Wang, P.-F. Li, D.-W. Fu, Z. Wang, S. Gao, K. Yang, J.-M. Liu, J. Li, Y. Yan and R.-G. Xiong, *Science*, 2017, **357**, 306.